Viscosity Behavior of Hydroxylated and Acetoacetylated Polyesters

Ramanuj Narayan,[1] D. K. Chattopadhyay,[1] K. V. S. N. Raju,[1] N. N. Mallikarjuna,[2] Sheetal S. Jawalkar,[3] Tejraj M. Aminabhavi[3]

[1]*Organic Coatings and Polymer Division, Indian Institute of Chemical Technology, Hyderabad 500 007, India*
[2]*Department of Chemistry, Alan G. MacDiarmid Laboratory for Innovative Research, University of Texas at Dallas, Richardson, Texas 75808*
[3]*Molecular Modeling Division, Center of Excellence in Polymer Science, Karnatak University, Dharwad 580 003, India*

Received 7 April 2005; accepted 23 June 2005
DOI 10.1002/app.23341
Published online in Wiley InterScience (www.interscience.wiley.com).

ABSTRACT: Viscosity studies on polyester polymers are important for governing their processing characteristics before their industrial application. In this study, the viscosity properties of hydroxylated polyesters with different diols and partially acetoacetylated polyesters with different amounts of ethyl acetoacetate were examined. The melt viscosities of these polymers were measured with different shear rates and at varying temperatures. The results were analyzed with the Williams–Landel–Ferry equation. In high-solid-coatings applications, an understanding about the surface properties and thermodynamic quantities, such as cohesive energy density, the solubility parameter, and the Flory–Huggins interaction parameter, are important. To evaluate these quantities, an atomistic simulation methodology based on Accelrys software was used, which provided insights into the structures of these compounds for further applications. © 2006 Wiley Periodicals, Inc. J Appl Polym Sci 100: 2422–2435, 2006

Key words: molecular modeling; polyesters; viscosity

INTRODUCTION

The viscosity properties of organic coatings are important in industrial applications. Probably, no paint or organic coatings dispersion is a true Newtonian system, but the non-Newtonian properties of these systems have been studied in terms of their viscosity characteristics.[1–4] However, low-molecular-weight oligomers are the basic components of formulations in high solids coatings, and hence, it is important to understand the melt-viscous properties of oligomers for any practical application. The importance of binder viscosity and thermodynamic factors that influence the formulation of high solid contents and the physical and mathematical aspects of the flow associated with the free volume of high solid contents have been investigated.[5–10] The temperature dependence of the viscosity of oligomeric butyl and methyl methacrylates in *m*-xylene was analyzed[11] by the famous Williams–Landel–Ferry (WLF) equation for a wide range of concentrations, temperatures, and oligomers. The viscosities of oligomers were found to depend on their structures, solvent viscosity, glass-transition temperature (T_g), solvent–oligomer interactions, temperature, and concentration. A simplified form of the WLF equation was used[12] to describe the viscosity of solutions of etherified melamine formaldehyde crosslinkers and high-solids polyester resins. Recently, the melt viscosity behavior of aliphatic hyperbranched polyesters with various molecular weights was studied,[13] and the flow activation energies (E_a's) were evaluated from the temperature dependence of the steady shear viscosity of the polymers. Jones[14] described the use of WLF and Arrhenius equations to study the temperature dependence of the viscosity of linear oligoester diols to determine how the chemical structure and shape of the oligomeric polyester resins affected their melt viscosities.

We undertook this study to examine the effect of structural variations in hydroxylated polyesters (HPs) with different diols and acetoacetylated products on their rheological properties at various shear rates and temperatures. The temperature dependence of the viscosity was analyzed with Arrhenius and WLF equations. However, measuring the important thermodynamic properties of such new polymers is time-con-

This article is Center of Excellence in Polymer Science communication #68.

Correspondence to: K. V. S. N. Raju (drkvsnraju@yahoo.com) or T. M. Aminabhavi (aminabhavi@yahoo.com).

Contract grant sponsor: Council of Scientific and Industrial Research (to R.N. as a Senior Research Fellow).

Contract grant sponsor: University Grants Commission, New Delhi; contract grant number: F1-41/2001/CPP-II (to T.M.A. for setting up the Center of Excellence in Polymer Science).

TABLE I
Components and Molar Ratios of the HPs

Component	HP code		
	HP100	HP200	HP300
NPG (mol)	4.40	—	—
CHDM (mol)	—	4.40	—
PD (mol)	—	—	4.40
AA (mol)	1.65	1.65	1.65
IA (mol)	1.65	1.65	1.65
TMP (mol)	0.7	0.7	0.7

suming and expensive. In recent years, the properties of polymers through atomistic simulation has been predicted, to a reasonable degree of success, with the computer-assisted Accelrys software.[15] Such attempts provided useful information on polymers in their condensed phases without a loss of detail on their chemical structures because it was difficult to understand such properties experimentally for the systems in this study. To understand the properties of the polyesters in their solid-state forms, atomistic simulation was carried out to compute the equilibrium conformation in the systems that were in a liquid state. However, through a powerful atomistic procedure, we brought the polymers sufficiently close to their thermodynamically realistic states and estimated their cohesive energy density (CED), Hildebrand solubility parameter (δ), and Flory–Huggins interaction parameter (χ) values and used this information to predict the properties of the compounds in their solid states. Such computations provided us with insights into the structures of the compounds in their solid states.

EXPERIMENTAL

Materials

The chemicals were purchased from different sources. Neopentyl glycol (NPG) and 1,4-cyclohexane dimethanol (CHDM) were obtained from Eastman Chemical Co. (New York). 1,3-Propane diol (PD) was purchased from Lancaster. Trimethylolpropane (TMP) was purchased from Aldrich (Milwaukee, WI), and adipic acid was purchased from S. D. Fine Chemicals (Mumbai, India). Isophthalic acid (IA) was purchased from SISCO (Mumbai, India), and ethyl acetoacetate (EAA) was purchased from Ranbaxy (Mumbai, India).

Synthesis of the HPs

The polymers used were prepared per a procedure explained previously.[16–19] Briefly, three HPs, HP100, HP200, and HP300, with the same hydroxyl value of 240, were synthesized by a conventional melt condensation process. The components and molar ratios used are reported in Table I. All of the components of a HP were put into a 2-L, four-necked, round-bottom flask equipped with a mechanical stirrer, a thermometer, a nitrogen inlet, and a Dean–Stark apparatus and were heated slowly until the mixture was agitated. The temperature was raised slowly and then maintained between 230 and 240°C. We followed the reaction by determining the acid value periodically. When it went down to less than 5, heating was stopped, and then, the mixture was cooled to ambient temperature.

Synthesis of acetoacetylated HPs

The synthesized HPs were transesterified with EAA to incorporate a β-ketoester group pendant to the polymer backbone. EAA was added to the HP melts at 80°C. The reaction temperature was raised to 140°C in about 2–3 h and then maintained until no distillate of ethanol was collected; ethanol was identified with gas chromatography. The stoichiometry of HP and EAA were adjusted to 10, 20, 30, 40, and 50% acetoacetylate of the available hydroxyl groups. The acetoacetylated HPs were coded as HP101–HP105 with 10–50% acetoacetylation of HP100. In a similar manner, acetoacetylated HPs derived from HP200 and HP300 were coded as HP201–HP205 and HP301–HP305, respectively. The chemical structures of the single HPs, say HP100, are shown in the Appendix. These structures were generated from the condensation product A (i.e., the reaction between NPG and adipic acid) and B (i.e., the reaction between NPG and IA), which condenses through the acid group of A and B, as shown in structure C. Therefore, the structure of HP100 was quite complex because it was a mixture of structures **I** to **VIII.** Similarly, the structures of HP200 and HP300 were quite complex. The physicochemical and thermal data on these compounds have been already reported.[18,19]

Determination of the viscosity

Before the viscosity measurements were performed, the HPs and acetoacetylated HPs were kept *in vacuo* at 60°C for 3–4 h, and then, they were cooled to room temperature. The viscosities of the neat HPs were determined in the temperature interval 30–80°C with an increment of 10°C with a Haake (Philadelphia, PA) rotational viscometer 2.1 system M5/SV2 (sensor SV2, measurement system M5, and instrumental factor A = 37.66, factor M = 4.450). The results of apparent viscosity, shear stress, and shear rate were obtained with the software supplied with the instrument. The viscosities of the pure HPs in the shear rate range 0.4–25 s^{-1} were Newtonian, but at high shear rates, they exhibited a marginal shear thinning behavior. A shear rate of 20 s^{-1} was maintained throughout the study.

WLF equation

The WLF equation[20] has been widely used to study the temperature dependence of viscosity for a wide range of polymers.[21] The simplified version of WLF equation that describes the relationship between the viscosity and T_g of an amorphous polymer is given by

$$\log \eta_T = \log \eta_{T_g} - \left[\frac{C_{1,g}(T - T_g)}{C_{2,g}} + (T - T_g) \right] \quad (1)$$

where η_T and η_{Tg} are the viscosities at the experimental temperature (in K) and glass-transition temperature (in K), respectively; T is the experimental temperature; T_g is the glass-transition temperature; and $C_{1,g}$ and $C_{2,g}$ are material constants. Equation (1), with some assumptions, can be used to describe the viscosity of the oligomers:

$$\log \eta_T = 12 - \left[\frac{A(T - T_g)}{B} + (T - T_g) \right] \quad (2)$$

where η_T is the viscosity at the experimental temperature of the measurement, A and B are material constants, and the number 12 is the viscosity at T_g, which was assumed to be 10^{12} Pa in the natural logarithmic scale.

Determination of the free volume and the expansion coefficient (α)

It is important for one to know the free volume and α of the polymers before envisaging applications of polymers in industrial sectors. The free volume at the glass-transition temperature (f_g) and α of the amorphous polymers[9] are related to $C_{1,g}$ and $C_{2,g}$ as

$$C_{1,g} = (2.303 f_g)^{-1} \quad (3)$$

$$C_{2,g} = \frac{f_g}{\alpha} \quad (4)$$

These equations are based on the assumption that free volume is a linear function of temperature and is given by

$$f_T = f_g + \alpha(T - T_g) \quad (5)$$

where f_T and f_g are the free volumes at the experimental temperature and the glass-transition temperature, respectively, and α is the difference between the thermal expansion coefficient above and below the T_g. Equation (1) is expected to hold good for all polymers throughout the temperature range between T_g and T_g + 100 K, with the upper limit corresponding to a fractional free volume of about 0.08. Equation (5) is assumed to be valid for plasticizers and solvents,[22] but it is very difficult to measure the viscosity at T_g. On the other hand, it is difficult to determine the true T_g thermodynamically because the magnitude of T_g depends on the method used for its determination.[23] It is, therefore, more convenient to express eqs. (1) and (5) in terms of another reference temperature, T_c, at which the viscosity would be easier to measure. The subscript g in eq. (1) can then be replaced by zero. Hence, the fractional free volume, α, and T_0 can be experimentally determined by the measurement of the viscosities of the oligomers at different temperatures with a modified form of eq. (1) given as

$$T - \frac{T_0}{\log\left(\frac{\eta_T}{\eta_0}\right)} = -\frac{1}{C_{1,0}(T - T_0)} - \frac{C_{2,0}}{C_{1,0}} \quad (6)$$

where η_0 is viscosity at T_0 and η_T is viscosity at T. Thus, if the viscosity of the polymer obeys the WLF relationship, a plot of $[T - T_0/\log(\eta_T/\eta_0)]$ versus $(T - T_0)$ gives a straight line, the slope of which allows one to calculate $C_{1,0}$ and the intercept $C_{2,0}$, and hence, f_0 and α can be calculated from eq. (4).

Arrhenius equation

The viscosity–temperature relationship of polymers and oligomers (without curing agents) can be characterized by the Arrhenius equation:

$$\ln \eta = \ln A - \frac{E_a}{RT} \quad (7)$$

where η and A are the melt viscosity and Arrhenius constant, respectively, that are characteristic of the resin and E_a, R, and T are the activation energy for viscous flow, universal gas constant, and absolute temperature, respectively. The previous relationship is applicable to a large number of polymer melts,[12,24] but we used eq. (2) to calculate the constants A and B. Equation (5) was used to calculate the free volume and α's, whereas eq. (7) was used to calculate the E_a values of the HPs and acetoacetylated HPs by regression analysis.

Atomistic simulation

In atomistic simulation, the properties of polymers in the condensed state can be predicted very accurately by the selection of an appropriate force field to obtain valuable information on the dynamics of polymer chains. Several force field approaches have been used to tackle such problems.[25–28] However, the viscosity properties of the polyesters in this work could not be directly related to the results of the simulation methodology because the polyesters in this study were mostly in the liquid state. However, atomistic simula-

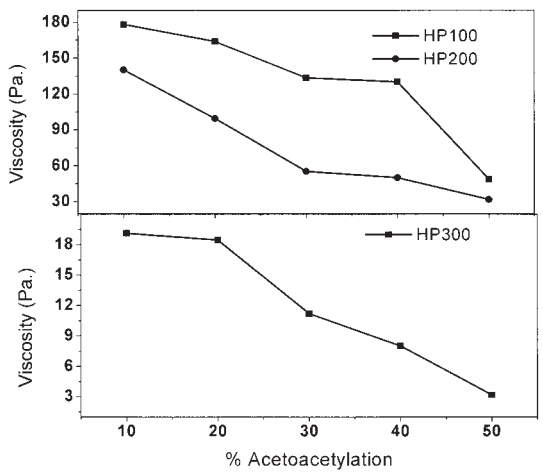

Figure 1 Effect of the temperature on the viscosity (at a shear rate of 24 s^{-1}) of HPs and acetoacetylated HPs: (a) HP100–HP105, (b) HP200–HP205, and (c) HP300–HP305.

tions helped us to understand the dynamics of the polymers in the condensed state, from which useful thermodynamic properties could be derived. Hence, in this study, for all the HPs *in vacuo*, that is, in their three-dimensional (3D) condensed bulk state, the nonbonded van der Waals interactions were computed between the atom pairs within a distance of 12 Å. With a COMPASS[29] force field approach, the CEDs and δs of the HPs were computed because these properties were not accessible experimentally on the systems developed in this study. In the COMPASS force field, the total potential energy (E) of the system is given by

$$E = E_b + E_0 + E_\phi + E_{oop} + E_{pe} + E_{vdw} + E_q \quad (8)$$

Here, the first four terms represent the bonded interactions, which correspond to the energies associated with the bond (E_b), bond angle bending (E_0), torsion angle rotations (E_ϕ), out of loop (E_{oop}), and potential energy (E_{pe}). The last two terms represent the nonbonded interactions, which consist of the van der Waals term (E_{vdw}) and the electrostatic force (E_q). E_{vdw} is described by the Lennard–Jones 6–12 potential, whereas the electrostatic energy is calculated from the partial charges of atoms in the system as estimated by the

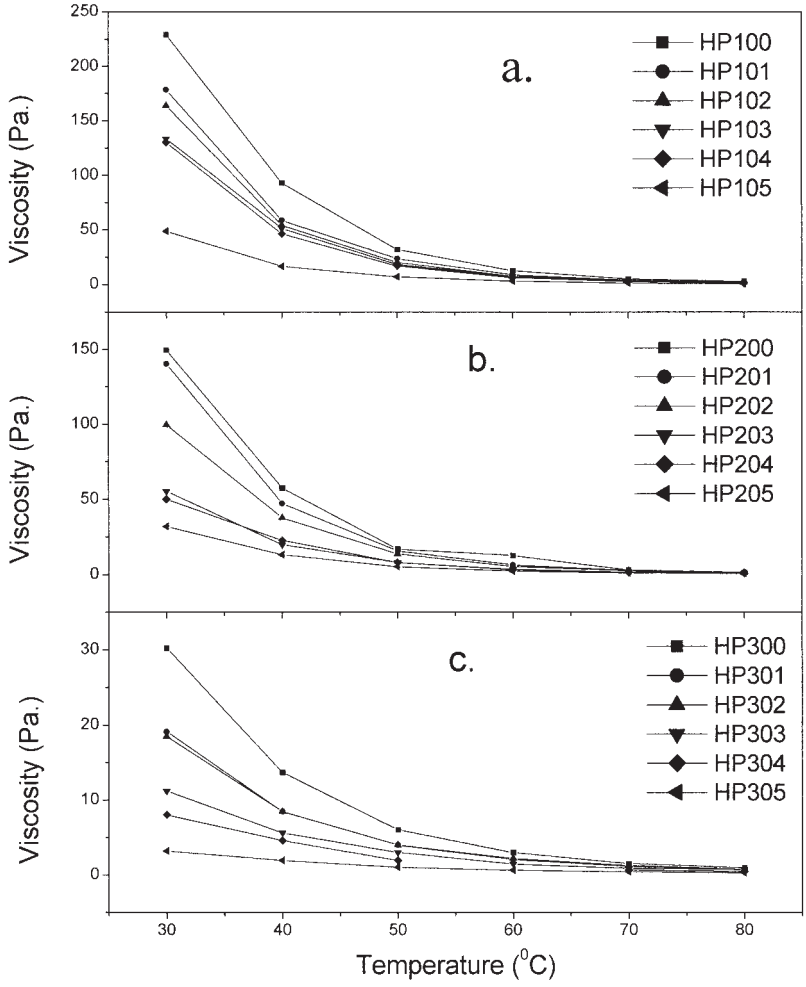

Figure 2 Effect of acetoacetylation on the viscosity (at 30°C and a shear rate of 24 s^{-1}) of HPs.

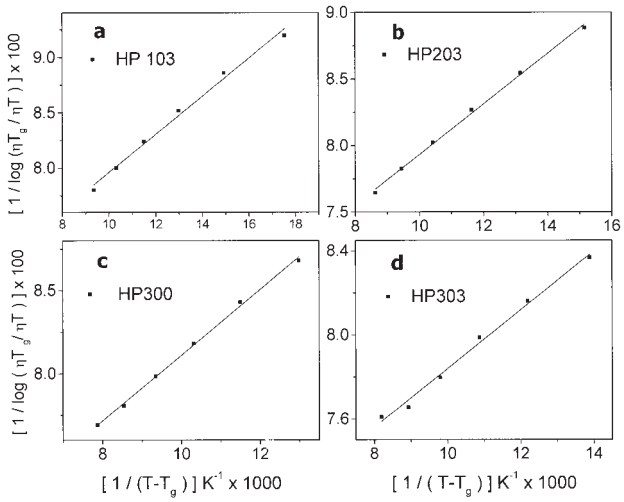

Figure 3 Representative temperature dependence plots of the viscosity data by WLF treatment [eq. (5)].

charge-equilibration method. To construct the cubic cell, the Theodorou and Suter method[30] was used because it calculates the long-range interactions more accurately.

The bulk amorphous state of the polyesters was built with cubic unit cells subjected to periodic boundary conditions. Simulations were performed with Discover molecular mechanics and dynamics simulation modules, supplied by Accelrys (Bangalore, India). The systems were built with a 3D periodicity and were equilibrated in the NVT (where N is number of atoms, V is constant volume, and T is constant temperature) ensemble at 298 K. This equilibration was usually done for 5 ps with the dynamics, which was followed by a data accumulation run lasting at least up to 100 ps, with the configurations saved every 5 ps. The detailed model construction procedure was described by different numbers of chains of polyesters in the unit cells. The density of the polyester was taken roughly as 1 g/cm^3. The initial amorphous structure was in a relatively high-energy state, and hence, before performing the atomistic calculations, we had to perform energy minimization; when the system approached close to minimum; then, the conjugate gradient method was used.[31] The simulation time depended on the number of atoms in the system, which was carried out until the total energy of the system was stabilized. The last few hundred picoseconds of the trajectory files were used to calculate δ, defined as the square root of CED, as well as χ with

$$\chi = \frac{z\Delta E_{mix}}{RT} \tag{9}$$

where ΔE_{mix} is energy of mixing; z is the coordination number, whose value for a cubic lattice model[32] was taken as 6; R is the molar gas constant (cal/mol); and T (298 K) is temperature (in K) at which the simulation was performed.

TABLE III
A and B Values of HP200 and its Acetoacetylated Counterparts

HP code	A	B	$(1 - \sigma^2)$
HP200	16.25	29.06	0.0177
HP201	16.46	29.86	0.0026
HP202	16.49	29.9	0.0007
HP203	16.56	31.38	0.0006
HP204	16.70	35.41	0.0023
HP205	17.02	38.35	0.0010

Surface energy (γ) calculations for the polyesters

Because of the widespread practical applications, the occurrence of polyester surfaces is important in several areas of coatings, adhesives, and sealants.[33] However, these data were not available with these systems, and hence, γ was calculated from the simulation procedure. The polyester system built initially was associated with a high energy, and hence, the systems were subjected to minimization, which made the system amorphous. After the cell construction and application of the dynamics, γ of the system was calculated with the CED data as[34]

$$\gamma = 0.75E_{coh}^{2/3} \tag{10}$$

where γ is the surface energy and E_{coh} is the cohesive energy density.

X-ray scattering curves

It is almost impossible to obtain the X-ray scattering data on the type of polyester systems developed in

TABLE II
A and B Values of HP100 and its Acetoacetylated Counterparts

HP code	A	B	$(1 - \sigma^2)$
HP100	14.22	12.24	0.0106
HP101	15.72	21.69	0.0013
HP102	15.81	26.32	0.0022
HP103	16.01	27.49	0.0028
HP104	16.04	26.99	0.0023
HP105	16.16	29.30	0.0014

TABLE IV
A and B Values of HP300 and its Acetoacetylated Counterparts

HP code	A	B	$(1 - \sigma^2)$
HP300	15.53	19.14	0.0001
HP301	15.54	21.71	0.0007
HP302	15.76	22.15	0.0019
HP303	15.93	26.63	0.0027
HP304	15.96	26.28	0.0002
HP305	16.30	32.24	0.0035

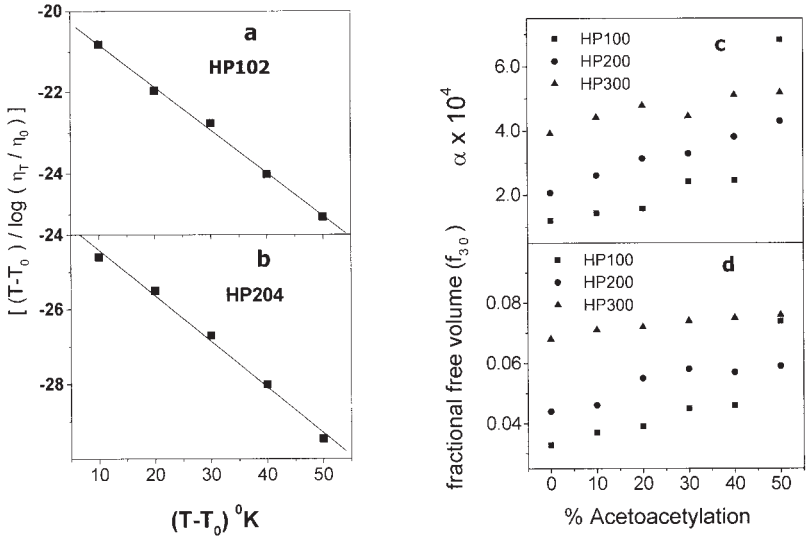

Figure 4 Representative temperature dependence plots of the (a, b) viscosity data by WLF treatment [eq. (6)] and (c, d) free volume and thermal α,.

this study. Hence, we used the atomistic simulation methodology to study the X-ray scattering of the compounds in their assumed solid states. To calculate the X-ray scattering curves of the amorphous polyester systems, we required as input all of the atoms in the system. Such calculations may be performed either on a single configuration or on a series of configurations. The actual procedure uses the Debye formula[35] to calculate the scattering curves with appropriate rigorous modifications to eliminate the effects of artificially imposed periodicity. The output results are the values of intensity versus either the scattering angle (θ) or the scattering vector ($\mathbf{q}$) given by[36,37]

$$q = \left(\frac{4\pi}{\lambda}\right)\sin\left(\frac{\theta}{2}\right) \tag{11}$$

where λ is the radiation wavelength. The scattering curve [$I(q)$] for the polymer is related by a Fourier transform operation to the radial distribution function. For an isotropic amorphous structure, the curve may be expressed as

$$I(q) = \sum_j \sum_k \frac{[f_j f_k(\sin qr_{jk})]}{qr_{jk}} \tag{12}$$

where q is the magnitude of the scattering vector, f_i is the form factor of j^{th} point, f_k is the form factor of k^{th} point, and r_{jk} is the distance between j^{th} and k^{th} points. The indices j and k extend over all atoms in the entire polymer chain. However, this experimental $I(q)$ may be used as a means of validating a force field. Thus, with the input atoms in the system, we performed the structural analysis for scattering X-rays.

RESULTS AND DISCUSSION

HP oligomers are quite complicated systems in the pure oligomeric phase due to a wide distribution of low-molecular-weight species (containing ester groups and primary hydroxyl groups) and hydrogen bond formation or self-association. A pure oligomer can be used as a reference point to discuss factors that affect viscosity because the oligomer comprises almost over half of the high solids. Factors such as molecular weight, molecular weight distribution, T_g, functional group content of the oligomers, solvent–oligomer interactions, concentration/viscosity relationships, and temperature affect the viscosity.[4] As reported earlier,[17–20] changes in the chemical structure of HPs due to the presence of different diol moieties and acetoacetyl groups have a significant influence on the molecular weight, polydispersity, and T_g of the HPs.

Effect of diol structures on the viscosity of HPs

The use of different diol structures in the HP backbones resulted in a substantial change in the viscosity. Figure 1 depicts the effect of diol structure variation and percentage acetoacetylation on the viscosity of the HPs at dif-

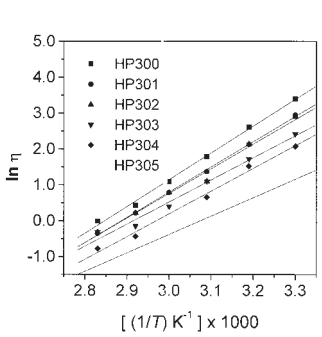

Figure 5 Representative plot of the Arrhenius equation to show the temperature dependence of the viscosity of HP 300 and the acetoacetylated HP 300 series.

TABLE V
E_a Values Calculated from the Arrhenius Equation

HP code	E_a (kJ/mol)	HP code	E_a (kJ/mol)	HP code	E_a (kJ/mol)
HP100	82.17	HP200	83.78	HP300	62.11
HP101	81.26	HP201	82.28	HP301	58.47
HP102	81.76	HP202	79.25	HP302	57.05
HP103	80.95	HP203	74.84	HP303	50.73
HP104	80.48	HP204	75.60	HP304	52.73
HP105	71.47	HP205	70.46	HP305	42.69

ferent temperatures. At 30°C, the viscosities of HP100, HP200, and HP300 were 229.1, 149.5, and 30.23 Pa, respectively. However, the structural variation in HP100, HP200, and HP300 was due to the presence of NPG, CHDM, and PD, respectively, in the polymers.

On the basis of molecular weight data, the viscosity of HP200 was expected to be higher than HP100 and HP300, but the viscosity of HP100 was found to be the highest. Although there was no discernable correlation between the viscosity and T_g, in general, an increase in T_g is associated with an increase in viscosity.[5,12] Because all the ingredients used in the HPs were the same except diol, this was mainly attributed to the differences in the T_g values of HP100, HP200, and HP300. Thus, the major factor contributing to the viscosity was the steric factor associated with the different diol structures. For HP100, the methyl groups of NPG caused steric hindrance for the movement of the HP segment on the application of shear, and hence, it exhibited the highest viscosity. On the other hand, for HP200, the 1,4-substituent on the cyclohexane ring helped in the slight freedom to segmental movement, and hence, its viscosity was lower than that of HP100. Comparatively, the linear structure of PD in HP300 provided the maximum freedom of movement on the application of shear to the HP segments, which in turn, resulted in the lowest viscosity.[12]

The results of Figure 1 were taken at a shear rate of 24 s^{-1}. A tremendous decrease in the viscosity of all of the HPs and acetoacetylated HPs with increasing temperature was found. With increasing temperature from 30 to 80°C, the viscosity of HP100, HP200, and HP300 decreased from 229.1 to 2.87, 149.5 to 1.31, and 30.23 to 0.99 Pa, respectively. Similarly, for all of the acetoacetylated HPs, a substantial reduction in viscosity was observed with increasing temperature. This effect was attributed to the moisture sensitivity of the compounds, which tended to decrease the viscosity with increasing temperature.

Effect of β-ketoester groups on the viscosity

Figure 2 shows the effect of percentage acetoacetylation on the viscosity of the HPs at different temperatures. Here, acetoacetylation, or the incorporation of β-ketoester groups, resulted in a significant reduction in the viscosity of the HPs. This was due to the replacement of more polar OH groups with less polar and bulky β-ketoester groups pendant to the polymer backbone, which in turn, resulted in chain separation

TABLE VI
Energy Components for the 3D Periodic Polyester Systems (in kcal/mol)

Polyester	Repeating units	E_{pe}	E_b	E_ϕ	E_0	E_{vdw}	E_q	E_{oop}
I	1	−72.9	6.2	−49.2	−2.9	12.6	−86.1	1.0
	4	−268.7	21.5	−162.5	−8.4	68.2	−348.9	2.7
II	1	71.4	9.4	14.1	−3.4	29.8	−10.1	1.1
	4	231.8	30.6	−1.4	−9.8	111.8	5.7	5.9
III	1	−7.2	11.3	−29.3	−4.6	38.2	−74.4	1.3
	4	43.3	189.6	−166.9	−13.0	129.2	−108.2	3.5
IV	1	41.1	10.0	−35.7	−5.1	32.3	−9.7	2.5
	4	73.6	33.7	−161.1	−13.6	129.6	−93.0	3.5
V	1	1.2	7.5	−47.3	−2.4	28.0	−19.1	0.5
	4	−41.9	22.7	−196.5	−9.5	99.5	−81.1	0.4
VI	1	58.6	6.4	−11.2	−2.1	28.3	5.2	1.2
	4	128.0	24.3	−118.1	−10.1	105.7	12.1	4.1
VII	1	16.9	8.8	−49.4	−3.1	36.5	−19.6	0.8
	4	85.4	31.0	−194.0	−12.5	133.9	−17.3	1.8
VIII	1	1.9	4.2	−23.6	−2.1	13.6	−6.0	0.1
	4	−29.2	15.9	−51.6	−6.8	49.9	−123.2	2.8

TABLE VII
CED, δ, and χ Values for the Polyesters

Polyester	Repeating unit	CED (cal/cm^3)	δ $(cal/cm^3)^{0.5}$	χ
I	1	76.54	8.75	0.77
	4	70.65	8.40	0.72
II	1	65.09	8.06	0.66
	4	70.29	8.40	0.71
III	1	69.68	8.35	0.71
	4	65.90	8.10	0.67
IV	1	75.18	8.67	0.76
	4	65.21	8.07	0.66
V	1	69.27	8.32	0.70
	4	68.39	8.27	0.69
VI	1	67.17	8.19	0.68
	4	68.52	8.28	0.69
VII	1	69.62	8.34	0.70
	4	69.06	8.31	0.699
VIII	1	71.45	8.45	0.72
	4	68.52	8.28	0.69

and a reduction of the autoassociative effect due to hydrogen bonding in the HPs.[38,39]

WLF equation

The temperature dependence of viscosity is important for understanding the free volume concept and for calculating E_a. Various forms of the WLF equation and modified forms of Arrhenius equations were used to study the temperature dependence of the viscosity of the oligomers and polymers. The viscosity data of all HPs measured at different temperatures and T_g of all of the HPs were fitted to eq. (2) with the original software (Version 5.0). All of the viscosity data were fit to a straight line with the correlation coefficient ($\sigma^2 \geq 0.99$), which suggested that viscosity data followed the WLF equation. Representative plots are shown in Figure 3. The calculated values of A and B with the values of $1 - \sigma^2$ are reported in Tables II–IV for HP100, HP200, and HP300 series with different amounts of acetoacetylation.

The temperature dependence of the viscosity can be affected by a number of parameters, including molecular weight, T_g, and polydispersity. However, this aspect was not studied in detail because the main objective of this study was to evaluate the application of the WLF equation to the temperature dependence on the viscosity. The constants A and B of the WLF equation, which were originally considered to be universal constants, were tested with the viscosity data of the HPs and acetoacetylated HPs at different temperatures without the use of any solvent, that is, with pristine HPs. The values of A and B obtained by the computation of the viscosity data in the WLF relation [eq. (2)] of the HPs showed that A varied from 14.22 to 17.02, and there was a wide variation in the values of the parameter B, that is, from 12.24 to 38.35 (see Tables II and IV). On the basis of these results, the parameter A can be considered a constant; its value was very near to that reported by Nielson[40] ($A = 17.44$ with a base logarithm 10 and $B = 51.6$). A fairly low value of $1 - \sigma^2$ indicated that the analysis of the viscosity data with the WLF equation, that is, eq. (2), produced good results. Similar results were reported by Jones,[14] who used oligoester resins without any solvent. However, the values of A and B suggested by Nielson[40] do not hold good for all polymer solutions and oligomers. Such variations in the values of A and B were also reported earlier by Wicks et al.[11]

One of the limitations of the WLF equation is that it is valid only in the temperature range between T_g and $T_g + 100$ K. We measured the viscosity of HPs in the temperature range 303–353 K (i.e., 30–80°C), and thus, results were obtained in the range $T_g + 31$ to $T_g + 128$ K and were largely outside the range at which the WLF equation is valid. Nonetheless, the representative WLF plots shown in Figure 3 were linear, which suggests the applicability of the WLF equation at temperatures up to $T_g + 128$ K. To validate this effect, we tested another form of the WLF relation [eq. (6)] to calculate the free volume and α, wherein we could observe linear trends typically, as shown in Figure 4(a,b). This further strengthened our argument that the HPs developed here followed WLF dependence. The free volume and α's calculated are displayed in Figure 4(c,d) and increased with decreasing viscosity. However, an increase in free volume might have allowed the chain ends to undergo segmental motions relatively readily, and hence, the viscosity was low.

Arrhenius equation

With the Arrhenius equation, the flow behavior of the polymers was studied to calculate E_a. The values of E_a were calculated from the plots of $\ln \eta$ versus $1/T$ from eq. (7). Representative plots are shown in Figure 5, and the E_a values of the HP100–HP300 series with different amounts of acetoacetylation are reported in Table V. The computer curve-fitting regression coefficient

TABLE VIII
γ Values for Polyesters with Four Repeating Units

Polyester with four repeating units	Cell width (Å)	γ $(cal/cm^3)^{2/3}$
I	16.50	12.8
II	16.97	12.8
III	17.96	12.2
IV	17.96	12.2
V	15.54	12.5
VI	16.82	12.6
VII	18.35	12.6
VIII	14.41	12.6

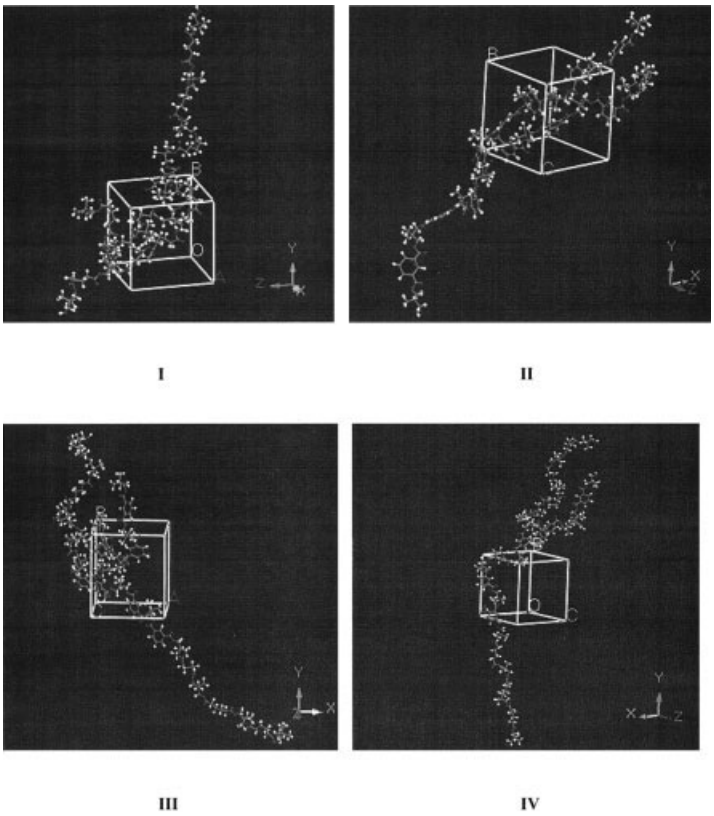

Figure 6 Simulated amorphous cell structure for polyesters **I–IV.** [Color figure can be viewed in the online issue, which is available at www.interscience.wiley.com.]

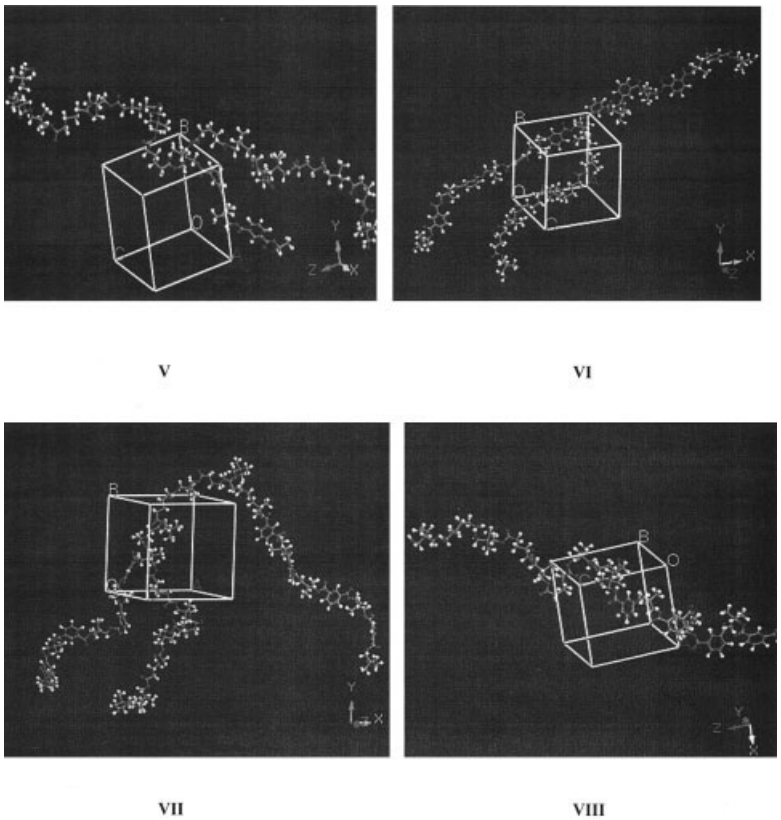

Figure 7 Simulated amorphous cell structure for polyesters **V–VIII.** [Color figure can be viewed in the online issue, which is available at www.interscience.wiley.com.]

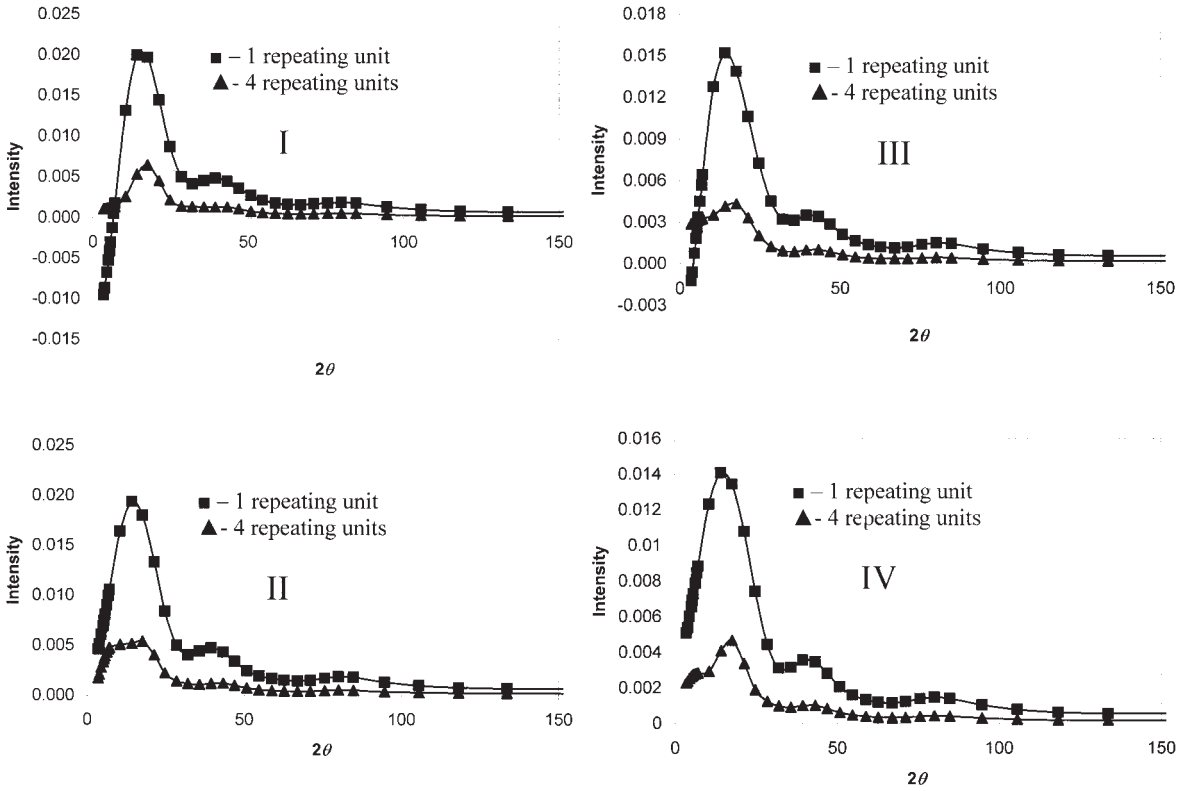

Figure 8 Representative X-ray scattering plots for polyesters **I–IV.**

(σ^2) was close to 1 and indicated the linearity of these plots. The E_a values of the linear HP300 series were quite lower than those of the nonlinear HP100 series (see Table V). The lower E_a for HP300 could have been due to its relatively linear structure as compared to HP100 and HP200 because PD was used as a major diol component. This was in agreement with the reported values of E_a found for linear polyethylene, which had the lowest E_a, which increased as the bulk of the side chain increased.[41] Even the substitution of a methyl group on the polymer side chain increased the E_a value because the resistance to flow increased. We inferred that the linear HP300s were likely to possess lower viscosities than the HP100s and HP200s if the other parameters of the formulations remained the same. It seems plausible that slender oligomers were able to move past one another more readily than bulkier ones. Linear HPs became partly aligned in a shear stress field and presented a smaller cross-section transverse to the stress than the nonlinear HPs, which offered lesser resistance to flow. Thus, they could flow into smaller holes between molecules in the liquid. A decrease in E_a with increasing acetoacetylation could have been due to a reduction in self-association between the chains through hydrogen bonding, which helped to decrease the potential energy barrier for the viscous flow.

Atomistic simulations

The potential energy decompositions as per eq. (8) calculated for the relaxed bulk structures are given in Table VI. The computed values of CED, δ, and χ are given in Table VII. For both the bulk structures with one and four monomer units of HPs, we observed that for all the systems, χ ranged between 0.6 and 0.7, whereas the average δ values were around 8 $(\text{cal/cm}^3)^{1/2}$. Generally, we observed that CED, δ, and χ values for higher structures were lower than those observed for single monomer units. Simulated bulk structures of HPs (given in Appendix) in their relaxed states generated from molecular dynamics simulations in the NVT ensemble are given in Figures 6 and 7. Here, the constant value refers to cell volume but not the effective volume occupied by the atoms in the periodic box. This procedure was successful for simulating the amorphous flexible polymers.

Molecular dynamics simulations were done for 100–200 ps, depending on the time required to achieve fluctuations in the potential and kinetic energies of less than 3% of the mean value, which did not deviate running along the integration time. However, depending on the size of the polyester, for which energy calculations were done, the cubic cell was developed in the software, and the edges of the cell varied in angstrom level, depending on the shape of the poly-

mer chain. For polyesters with one monomer unit, the cubic cell varied from 9 to 12 Å, whereas for polyesters with four monomer units, the cell size was between 14 and 18 Å. For longer chains, the time used for optimization was greater (70–90 min), whereas that for shorter chains was less (1–5 min). The cohesive energy densities obtained from the simulation studies were almost in the same range, that is, 61–76 cal/cm^3. χ values for all of the structures were between 0.62 and 0.77. γ values calculated for individual polyesters ranged between 12.2 and 12.8 (cal/cm^3)$^{2/3}$ (see Table VIII). However, at this stage, we could not make any connection between the viscosity trends of the oligomers and the simulation results because the latter were computed with the assumption of the solid forms of the same polyesters.

X-ray scattering

From the intensity plots of polyesters with one and four repeating units, we found that the maximum peak moved toward a smaller q. When the amplitudes and the corresponding wavelengths presented in Figure 8 were compared for the two systems at the same time step, we observed that the intensity of polyester was higher for a single unit than for four units. The amplitude in all cases was displaced toward a smaller q, which indicated higher peaks at the beginning due to thermal fluctuations and that the polyesters were in the amorphous state.

CONCLUSIONS

HPs (HP100, HP200, and HP300) differing in their diol structures were synthesized and acetoacetylated with different percentages of substitution of the available hydroxyl groups. Viscosity characterizations of all of the polyesters and acetoacetylated HPs were carried out at different temperatures. The diol structure variation and acetoacetylation resulted in a reduction in the viscosity values of the HPs. All of the HPs followed Arrhenius and WLF temperature dependence of the viscosity. However, at this stage, we could not relate the experimental results in their melt forms with those of the atomistic simulation results because the simulations were done in their amorphous solid states; yet, it is important to know that atomistic simulation procedures accurately predicted the surface properties and CED and δ values of the systems in addition to the χ values, which otherwise would have been difficult to obtain from experiments because the polyesters in this study were in the liquid state. X-ray scattering plots for all of the polyesters were generated, and the representative minimized structures are presented.

APPENDIX

For the structures of polyester HP100, units x and y of the structures could be any numbers from 0 to ∞, but the molecular weights of the polyesters were around 1000–1500. The values of x and y were taken between 1 and 4 units only during the simulation procedure. Similarly, for HP200 and HP300, only the NPG part was replaced by CHDM for HP200 and PD for HP300.

For structure C, structure A or B condensed through the acid group of A or B:

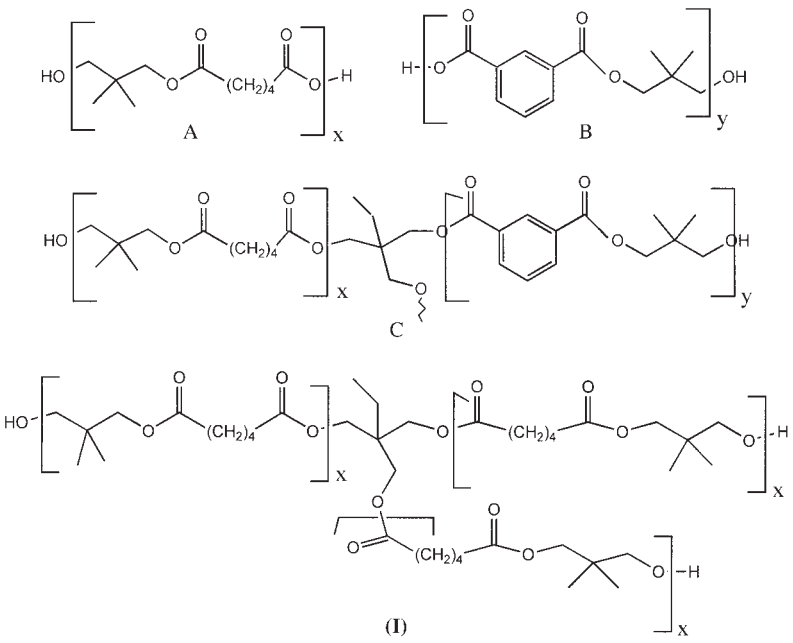

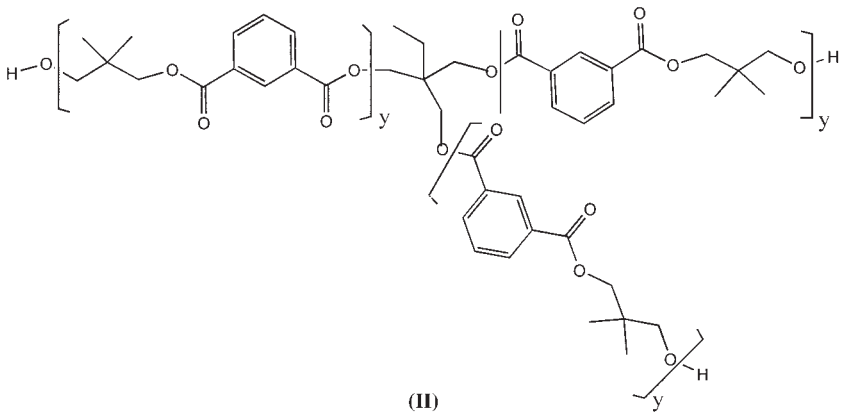

(II)

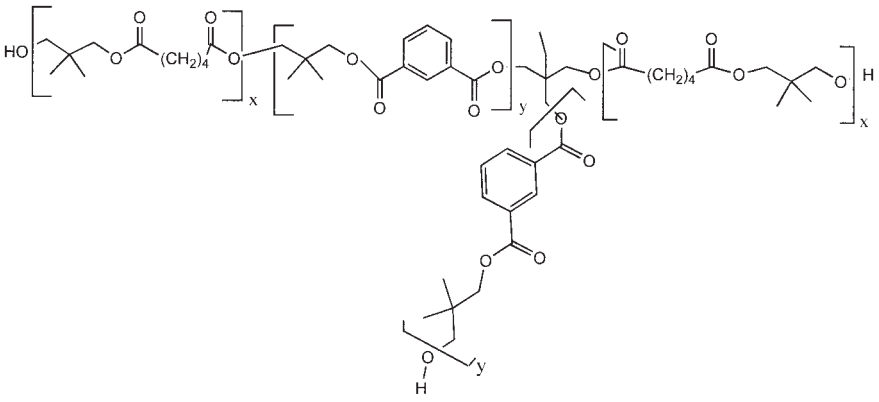

(III)

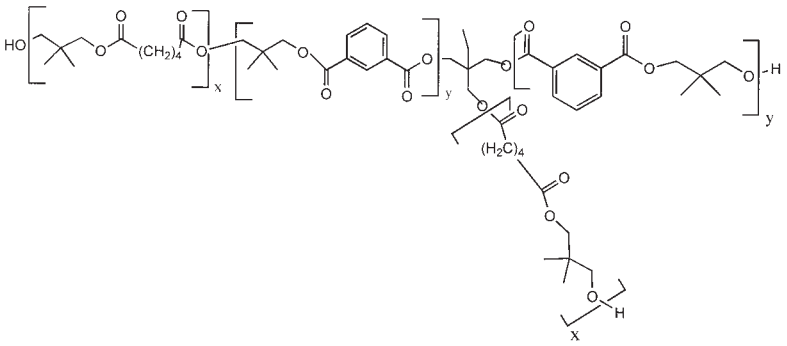

(IV)

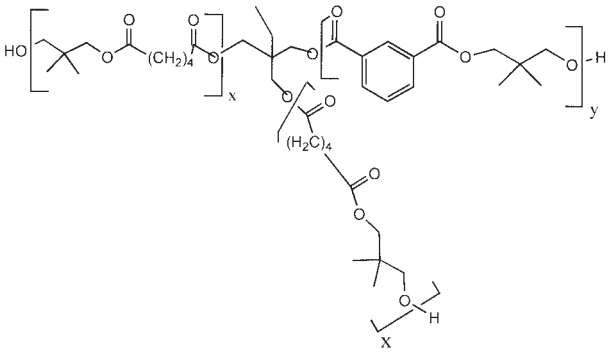

(V)

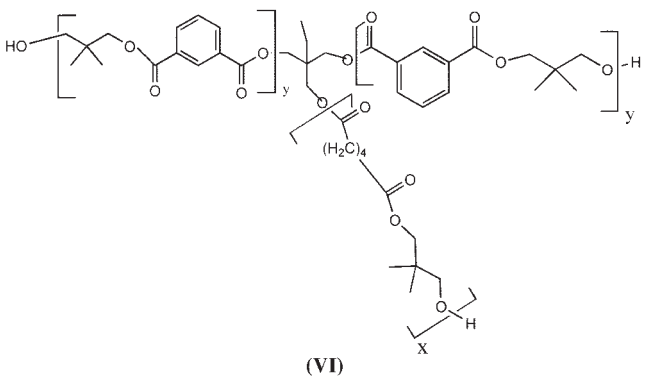

(VI)

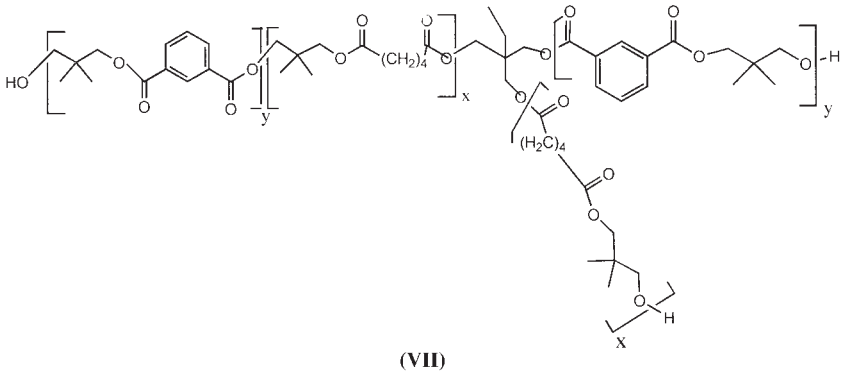

(VII)

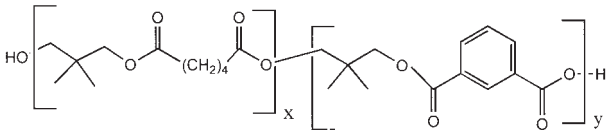

(VIII)

This research represents a collaborative effort between two institutions, the Indian Institute of Chemical Technology and the Center for Excellence in Polymer Science, under the Memorandum of Understanding.

References

1. Haseebuddin, S.; Raju, K. V. S. N.; Yaseen, M. J Appl Polym Sci 1997, 66, 1343.
2. Haseebuddin, S.; Raju, K. V. S. N.; Yaseen, M. J Appl Polym Sci 1996, 59, 29.
3. Raju, K. V. S. N.; Krishna, D.; Rama Devi, G.; Reddy, P. J.; Yaseen, M. J Appl Polym Sci 1993, 48, 2101.
4. Kok, C. M.; Rudin, A. Euro Polym J 1982, 18, 363.
5. Hill, L. W.; Wicks, Z. W., Jr. Prog Org Coat 1982, 10, 55.
6. Wicks, Z. W., Jr. J Coat Technol 1986, 58(743), 23.
7. Schoff, C. K. Prog Org Coat 1976, 4, 189.
8. Erickson, J. R. J Coat Technol 1976, 18(620), 61.
9. Toussaint, A.; Szigetvari, I. J Coat Technol 1987, 59(750), 49.
10. Bauer, D. R.; Briggs, L. M. J Coat Technol 1984, 56(716), 87.
11. Wicks, Z. W., Jr.; Jacobs, G. F.; Lin, I.-C.; Urruti, E. H.; Fitzgerald, L. G. J Coat Technol 1985, 57(725), 51.
12. Hill, L. W.; Kozlowski, K.; Sholes, R. L. J Coat Technol 1982, 54(692), 67.
13. Hsieh, T. T.; Tiu, C.; Simon, G. P. Polymer 2001, 42, 1931.
14. Jones, F. N. J Coat Technol 1996, 68, 28.
15. Accelrys Software. MS Modeling Getting Started; San Diego, 2004.
16. Narayan, R.; Raju, K. V. S. N. Prog Org Coat 2002, 45, 59.
17. Narayan, R.; Chattopadhyay, D. K.; Sreedhar, B.; Raju, K. V. S. N. J Mater Sci 2002, 37, 4911.
18. Narayan, R.; Chattopadhyay, D. K.; Sreedhar, B.; Raju, K. V. S. N.; Mallikarjuna, N. N.; Aminabhavi, T. M. J Appl Polym Sci 2005, 97, 1069.
19. Narayan, R.; Chattopadhyay, D. K.; Sreedhar, B.; Raju, K. V. S. N.; Mallikarjuna, N. N.; Aminabhavi, T. M. J Appl Polym Sci 2005, 97, 518.
20. Williams, M. L.; Landel, R. F.; Ferry, J. D. J Am Chem Soc 1955, 77, 3701.
21. Kumar, N. G. J Polym Sci Part D: Macromol Rev 1980, 15, 255.
22. Bueche, F. Physical Properties of Polymers; Wiley-Interscience: New York, 1962; p 57.
23. Toussiant, A.; Legras, R. Prog Org Coat 1976, 4, 251.
24. Patton, T. C. Paint Flow and Pigment Dispersion; Wiley-Interscience: New York, 1979; pp 93, 103.
25. Sun, H.; Ren, P.; Fried, J. R. Comput Theor Polym Sci 1998, 8, 229.
26. Meirovitch, H. J Chem Phys 1983, 79, 502.
27. Mattice, L. Macromolecules 1992, 25, 4942.
28. Rigby, D.; Sun, H.; Eichinger, B. E. Polym Int 1997, 44, 311.

29. Rappe, A. K.; Goddard, W. A. J Phys Chem 1991, 95, 3358.
30. Theodorou, D.; Suter, U. Macromolecules 1985, 18, 1467.
31. Spyriouni, T.; Vergalati, C. Macromolecules 2001, 34, 5306.
32. Flory, P. J. Principles of Polymer; Cornell University Press: Ithaca, NY, 1953.
33. Feast, W. J.; Munro, H. S. Polymer Surfaces and Interfaces; Wiley: New York, 1987.
34. Ijantkar, A.; Natarajan, U. Polymer 2004, 45, 1373.
35. Debye, P. W. Ann Phys 1915, 46, 809.
36. Press, W. H.; Flannery, B. P.; Teukolky, S.; Vetterling, W. T. Numerical Recipes; Cambridge University Press: Cambridge, England, 1987.
37. Witzeman, S. J.; Nottingham, D. W.; Rector, F. D. J Coat Technol 1990, 62, 101.
38. Clemens, R. J.; Rector, F. D. J Coat Technol 1989, 61, 83.
39. Vogt-Birnbrich, B. Prog Org Coat 1996, 29, 31.
40. Nielson, L. E. Polymer Rheology; Marcel Dekker: New York, 1977; p 33.
41. Eyring, H. J. Chem Phys 1936, 4, 283.